Available online at www.sciencedirect.com
ScienceDirect
Scripta Materialia 56 (2007) 1027–1030
Scripta MATERIALIA
www.elsevier.com/locate/scriptamat

Mixed-mode cleavage front branching at a high-angle grain boundary

Jin Chen and Yu Qiao*

Department of Structural Engineering, University of California at San Diego, La Jolla, CA 92093-0085, United States

Received 15 December 2006; revised 23 February 2007; accepted 1 March 2007
Available online 28 March 2007

In a previous study it was observed that a cleavage front can penetrate through a high-angle grain boundary in either regular or irregular mode. In this article, we report the third mode, which has a self-similar characteristic. In this mode, the cleavage front branches into a number of segments and the breakthrough points are in clusters, which can be regarded as the combination of regular and irregular processes. A first-order analysis is performed to estimate the boundary fracture resistance.

Keywords: Cleavage; Grain boundaries; Fracture

A major effort for improving fracture toughness of engineering materials is to understand the role of grain boundaries in the failure process [1–7]. For a polycrystalline material, e.g., a low-carbon steel at the lower shelf of the brittle-to-ductile transition region that often fails by transgranular cracking, grain boundaries offer important resistance to crack advance [8]. For instance, it has long been known that overcoming a few grain boundaries by a grain-sized microcrack can lead to catastrophic failure [9,10].

Once a cleavage crack passes through a high-angle grain boundary, its fracture surface must shift to the cleavage plane of the new grain, which is misorientated from that of the grain behind the boundary by a twist angle, θ, and a tilt angle, ψ. The two misorientation angles, together with a rotation angle and two parameters describing the orientation of the grain boundary plane, characterize the grain boundary structure [11]. For relatively ductile materials, while cleavage-like fracture can occur inside grains, the dominant factor of fracture resistance is the work of separation of grain boundaries [12]. In this case, a cleavage crack overcomes a grain boundary by shearing it apart. While each fracture facet is quite smooth, the overall fracture-surface roughness is determined by the facet misorientations.

In "purely" brittle materials, the crack–boundary interaction is more complicated. According to a recent study on iron–silicon alloys and low-carbon steels [13–16], as a cleavage front transmitted across a grain boundary, it was broken down into a number of segments. Each front segment penetrated into the grain ahead of the boundary somewhat independently. Due to the crystallographic misorientation, the crack front segments were no longer in the same plane. A set of parallel terraces were formed, and the terrace borders were eventually separated apart via secondary fracture, which could be observed on fracture surface as river markings, and will be referred to as cleavage ridges in the following discussion. Depending on the distribution of crack front segments, there were two possible breakthrough modes: the regular mode and the irregular mode. In the regular mode, the breakthrough points (BTP), the locations at which the crack front segments penetrated across the boundary, were close to each other and distributed along the boundary quasi-periodically, with the most probable distance around 2–3 μm. If the grain boundary strength was relatively weak, the grain boundary fracture resistance was dominated by the critical condition of unstable crack front advance, which was related to the competition between the increases of the local fracture resistance and the effective crack growth driving force [17,18]; otherwise, the crack trapping effect of the persistence grain boundary islands (PGBI) played a critical role [19]. In the irregular mode, the crack front penetrated into the second grain at only a small number of BTPs, which were far and few between. The BTP distance was usually larger than 50–100 μm. Since the grain boundary area in between the BTPs was wide, quite

* Corresponding author. Tel.: +1 858 534 3388; e-mail: yqiao@ucsd.edu

1359-6462/$ - see front matter © 2007 Acta Materialia Inc. Published by Elsevier Ltd. All rights reserved.
doi:10.1016/j.scriptamat.2007.03.002

often it could not be directly separated apart, and thus offered additional fracture resistance. The crack front might go back from the grain ahead of the boundary to the grain behind the boundary, creating local crack propagation loops, and consequently the fracture surface was relatively rough [20].

In this article, we report another mode of crack front transmission across a high-angle grain boundary, which will be referred to as the intermediate mode in the following discussion. It can be regarded as the combination of the regular mode and the irregular mode. We also analyze the associated grain boundary fracture resistance. The result shows that the intermediate mode can be triggered by a small increase in local crack-tip stress. While it is less energetically favorable than the regular mode, it leads to a reduced grain boundary resistance compared with the irregular mode.

Figure 1 shows a cleavage crack overcoming a high-angle grain boundary in the intermediate mode in an iron–3 wt.% silicon alloy. The details of the experiment have been discussed elsewhere [15]. It can be seen that in the grain ahead of the boundary, the fracture surface is broken down into a number of sections. Each section corresponds to a breakthrough zone (BTZ) at the boundary. Inside each BTZ there are a number of BTPs, leading to the formation of smaller river markings. Note that this structure is self-similar. The features of BTZs are quite similar to those of BTPs, except that the length scale is larger. The self-similar crack front penetration process is depicted in Figure 2(a). Similar to that in the regular mode, in most of the grain boundary the crack front transmits from the grain behind the boundary at BTPs that are closely aligned. However, the BTPs are self-organized into a number of groups. Each group forms a BTZ. If the fine features, i.e., the cleavage ridges between the BTPs, are ignored, each BTZ resembles a BTP, as if the BTP distance were large. In the iron–silicon alloy under investigation, the BTP distance, w, was around 2–3 μm, and the BTZ width, w^*, was 20–40 μm.

The primary fracture surface produced by the front segment penetrating at a BTP is the cleavage plane of the grain behind the boundary, with a twist misorienta-

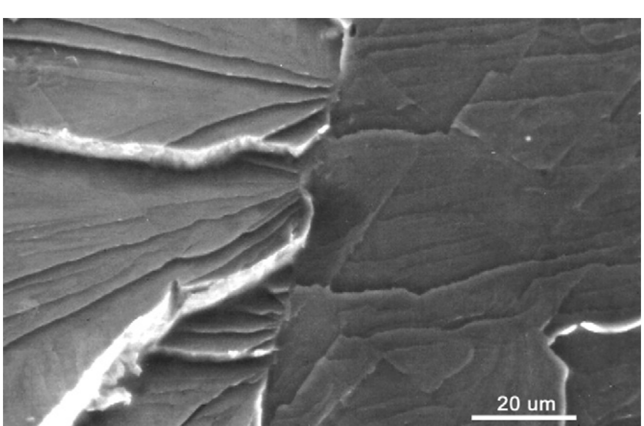

Figure 1. SEM microscopy of self-similar cleavage front branching across a high-angle grain boundary in an iron–3 wt.% silicon alloy. The crack propagates from the right to the left.

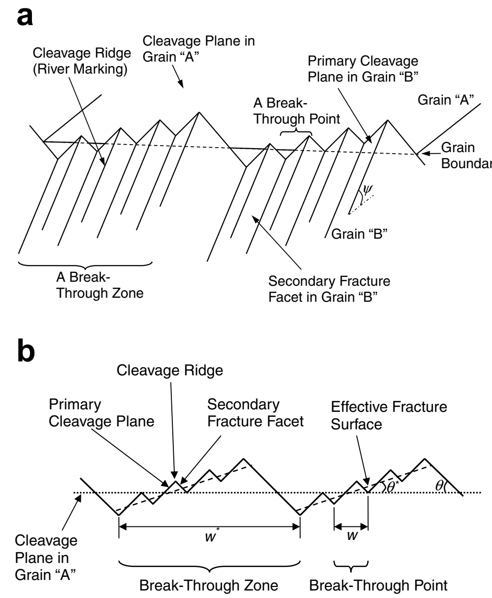

Figure 2. Schematic diagrams of hierarchical cleavage front transmission process across a high-angle grain boundary: (a) the three-dimensional view and (b) the end view, normal to the grain boundary plane from grain “B” to “A”.

tion angle of θ, as shown in Figure 2(b). The secondary fracture facets, according to the fractography study, are neither normal to the horizontal plane (the nominal fracture surface) nor normal to the primary cleavage plane, indicating that they are separated by mixed mode-II fracture and shearing, as well as plastic bending of ligaments caused by undercutting [15]. The river markings (cleavage ridges) indicate the profiles of advancing crack front segments. The BTP array in a BTZ form a fracture facet, which is misoriented by an angle of θ^*. Note that θ^* is determined not by the crystallographic orientation, but by the width and the relative height of BTZ, and usually $\theta^* \neq \theta$.

In order to analyze the mechanism of formation of BTZ, it is important to understand the grain boundary fracture resistance. If the crack front passes through the boundary in regular mode, the grain boundary resistance can be calculated as [15]:

$$G_w = G_{sc}\left[\frac{\sin\theta + \cos\theta}{\cos^2\psi} + C\frac{\sin\theta \cdot \cos\theta}{\cos\psi}\right], \tag{1}$$

where $G_{sc} = 850\ \mathrm{J\,m^{-1}}$ is the fracture resistance of a crystallographic plane and $C = \beta k w/(4G_{sc})$ is a material parameter, with $\beta = 2$ being the geometry factor of penetrating crack front segment and $k = 144$ MPa the effective shear strength. When w is set to the most probable value of 2.5 μm, $C = 0.25$ and the result of G_w fits well with the experimental measurements [13,15]. Since, in a BTZ, the crack front breaks through the boundary locally in regular mode, the local boundary resistance can be taken as G_w.

In the intermediate breakthrough mode, in addition to G_w, extra grain boundary areas associated with the misorientation of fracture surface of BTZ must also be separated apart. The extra area consists of the grain boundary in the central sections of BTZs and the grain boundary in the transition zones between BTZs, i.e., the grain boundary areas across major river markings. The former can be separated quite smoothly as the BTPs are formed, and therefore the associated resistance can be assessed using a similar method as G_w, i.e.,

$$G_{we} = G_{sc}\left[\frac{\sin\theta^* + \cos\theta^*}{\cos^2\psi} + C^*\frac{\sin\theta^*\cdot\cos\theta^*}{\cos\psi}\right]. \quad (2)$$

In Eq. (2), it is assumed that the behavior of the crack front in the central part of a BTZ is similar to that in a BTP only at a larger length scale, with θ^* and C^* being analogs to θ and C, respectively, $C^* = \beta^* k w^*/(4G_{sc})$; and β^* being the geometry factor of the overall crack front in a BTZ. Since the grain boundary shearing does not change with the features in fracture plane, at the first-order approximation level β^* can be assumed to be the same as β.

The grain boundary areas at BTZ borders are relatively difficult to fail. From Figure 1, it can be seen that significant ligament bending and shearing are involved in the final separation of fracture surfaces. That is, they act as reinforcements bridging across fracture flanks, which can be taken into account by using a crack trapping model [19]:

$$G_{ct} = G_w\left\{\left(1-\frac{D}{w^*}\right) + \left[1.7 + 2.4\frac{D}{w^*} + 0.1\left(\frac{D}{w^*}\right)^2\right]\right\}^2\left(\frac{D}{w^*}\right), \quad (3)$$

where D is the width of the bridging grain boundary area associated with cleavage ridges, with the average value about 1 μm. Since both the grain boundary areas in the central parts of BTZs and at cleavage ridges must be separated apart before the grain boundary is fully overcome, the effective grain boundary fracture resistance should be taken as the larger one of them:

$$G_{gb} = \max\{G_{ct}, G_{we}\}. \quad (4)$$

Figure 3 shows the numerical results of Eq. (4), where both the twist and tilt crystallographic misorientation angles are taken as 20°, close to their average values. The dotted line is for the reference grain boundary resistance, G_{ws}, which is calculated using Eq. (1) by setting $w = w^*$. It is the grain boundary resistance if the crack front broke through the boundary in irregular mode with the BTP distance the same as the BTZ distance. When the BTZ distance is relatively small, $G_{ct} > G_{we}$, i.e., overcoming the crack trapping effect of cleavage ridges is more difficult than the "regular" crack front transmission. Thus, the crack trapping effect dominates the overall grain boundary fracture resistance. When the BTZ distance is relatively large, $G_{ct} < G_{we}$, indicating that the influence of large river markings is negligible, and therefore the critical condition of unstable crack front advance is dominated by the fine fracture-surface features. At the critical value of w^*_{cr}, $G_{ct} = G_{we}$ and G_{gb} reaches the minimum value, G_{cr}, i.e., it is most energetically favorable for the crack front to overcome the grain boundary. With a given θ^*, when the initial BTZ distance is larger than w^*_{cr}, new BTZs tend to be formed by separating larger BTZs into smaller ones, and thus w^* decreases. Similarly, if initially BTZ is close to each other, adjacent BTZs may merge into larger ones so that

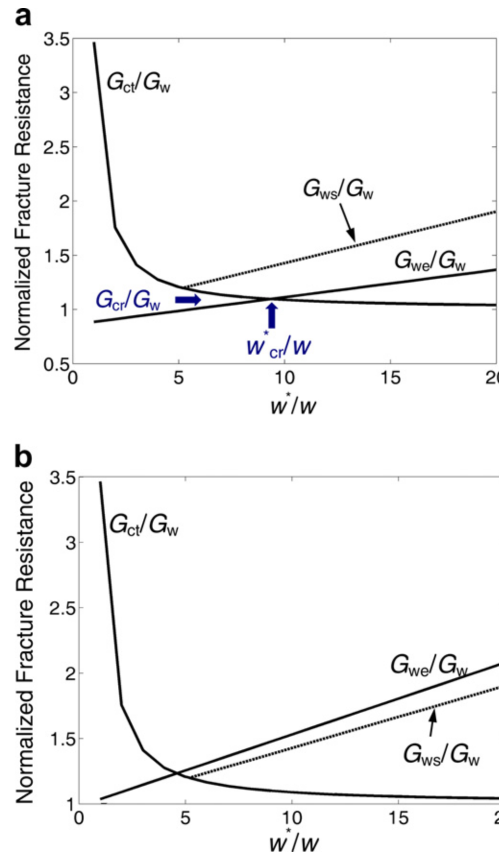

Figure 3. The fracture resistance as a function of the width of the BTZ, w^*: (a) $\theta^*/\theta = 0.5$ and (b) $\theta^*/\theta = 1.2$.

w^* increases. Eventually, at w^*_{cr}, the crack front transmission can occur once the nominal energy release rate reaches the critical value.

When $\theta^* < \theta$, as shown in Figure 3(a), G_{cr} is smaller than the irregular-mode grain boundary resistance, G_{ws}. Under this condition, by forming BTP clusters, i.e., BTZs, the energy barrier for the crack front to transmit across the grain boundary is lowered, and therefore the intermediate mode is more energetically favorable. When $\theta^* > \theta$, as shown in Figure 3(b), G_{cr} is larger than G_{ws}, indicating that the grain boundary can be more easily overcome in irregular mode. This was confirmed by the experimental observation that at all the intermediate-mode grain boundaries the effective twist angles of fracture surfaces were always smaller than the actual twist angles of crystallographic planes.

Note that in all the cases $G_{cr}/G_w > 1$, i.e., the most energetically favorable mode is the regular mode. In a previous investigation [14], we attributed the formation of irregular BTPs to the jerky nature of crack advance and the associated non-uniform front–boundary interaction. In this framework, according to the above discussion, if the uniform development of BTPs along the entire boundary is possible, the grain boundary will be passed through in regular mode. Otherwise, e.g., if the formation rate of BTPs is relatively small or the increase rate of local stress intensity is relatively high, the regular mode becomes difficult. If θ^* tends to be large, the irregular mode would dominate. If $\theta^* < \theta$, the intermediate

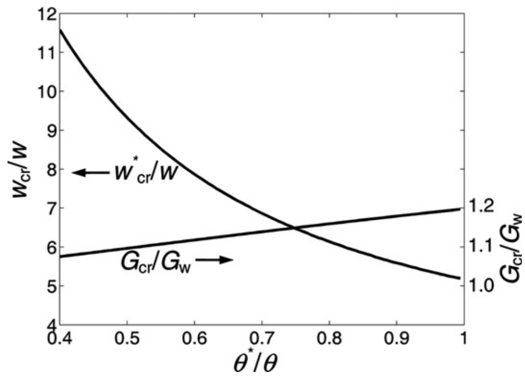

Figure 4. The effective fracture resistance and the optimum BTZ width as functions of the BTZ twist angle.

mode is more likely to take place, i.e., while the BTPs are close to each other, they are self-organized in clusters, resulting in the formation of BTZs.

The factors that govern θ^* cannot be analyzed via fractography study. In fact, in order to minimize the grain boundary fracture resistance, θ^* should be nearly zero, and thus the intermediate mode converges to the regular mode. The causes of the intermediate mode must be related to the kinetics of crack front behavior, such as the rate of increase of local stress intensity along the wavy crack front. Figure 4 shows that, as θ^* varies in a broad range, the effective grain boundary fracture resistance, G_{cr}, does not change much. When θ^*/θ increases from 0.4 to 1 by more than 100%, although the BTZ width, w^*_{cr}, largely decreases by a factor of more than 2, the increase in G_{cr} is only around 10%. Therefore, even a small increase in local crack-tip stress field may trigger the intermediate mode, causing grouping of BTPs. For the iron–silicon alloy investigated in the experiment [13–16], the numerical result is consistent with the observation that w^*_{cr} was about $10w$ and θ^*/θ was around 0.5.

To summarize, in previous studies, we analyzed the regular mode and the irregular mode of crack front transmission across high-angle grain boundaries. In this article, we discuss another mode – the intermediate mode – which can be regarded as a combination of them. The crack front breaks through the boundary at a number of BTPs closely distributed along the boundary. The BTPs form clusters, and each cluster leads to the formation of a breakthrough zone. The BTZ behavior is quite similar to the BTP behavior, except that the length scale is larger, exhibiting a self-similar characteristic. According to an analysis of grain boundary fracture resistance, the intermediate mode is more energetically favorable than the irregular mode when the overall fracture-surface twist angle is smaller than the twist angle of crystallographic planes. There exists an optimum BTZ width at which the energy barrier to crack front advance is minimum. The intermediate mode can be triggered by a small increase in local crack-tip stress level.

This work was supported by The Office of Basic Energy Science, The Department of Energy under Grant No. DE-FG02-05ER46195, for which the authors are grateful to Dr. Yok Chen.

[1] J.F. Knott, in: K.S. Chan (Ed.), Proc. of Cleavage Fracture: George R. Irwin Symp., TMS, Warrendale, PA, 1997. pp. 171.
[2] P. Kotowski, Int. J. Fracture 141 (2006) 269.
[3] J.A. Wert, Scripta Mater. 49 (2003) 607.
[4] I. Chasiotis, W.G. Knauss, J. Mech. Phys. Solids 51 (2003) 1533.
[5] S.W. Cho, K. Jonnalagadda, I. Chasiotis, Fatigue Fract. Eng. Mater. Struct. 30 (2007) 21.
[6] K. Nakagawa, T. Kanadani, N. Nagaoka, A. Sakakibara, G. Itoh, J. Jpn. Inst. Met. 70 (2006) 897.
[7] G. Odermer, G. Henaff, B. Journet, Scripta Mater. 54 (2006) 51.
[8] R.O. Ritchie, J.F. Knott, J.R. Rice, J. Mech. Phys. Solids 21 (1973) 395.
[9] C.L. McMahon, M. Cohen, Acta Metall. 13 (1965) 591.
[10] J.F. Knott, A.H. Cottrell, J. Iron Steel Inst. 201 (1963) 249.
[11] P.E.J. Flewitt, R.K. Wild, Grain Boundaries: Their Microstructures and Chemistry, John Wiley and Sons, New York, 2001.
[12] F.A. McClintock, in: K.S. Chan (Ed.), Proc. of Cleavage Fracture: George R. Irwin Symp., TMS, Warrendale, PA, 1997. pp. 81.
[13] A.S. Argon, Y. Qiao, Philos. Mag. A 82 (2002) 3333.
[14] Y. Qiao, A.S. Argon, Mech. Mater. 35 (2003) 129.
[15] Y. Qiao, A.S. Argon, Mech. Mater. 35 (2003) 313.
[16] Y. Qiao, A.S. Argon, Mech. Mater. 35 (2003) 903.
[17] Y. Qiao, Mater. Sci. Eng. A 361 (2003) 350.
[18] Y. Qiao, X. Kong, Mater. Lett. 58 (2004) 3156.
[19] X. Kong, Y. Qiao, Fatigue Fract. Eng. Mater. Struct. 28 (2005) 753.
[20] Y. Qiao, J. Mater. Sci. Technol. 21 (2005) 338.